MINER: Three-Dimensional Multi-Group Finite-Difference and Nodal Method for CANDU® Applications[1]

B. Phelps[a], W. Shen[a] and E. Varin[b]
[a]Atomic Energy of Canada Limited, Mississauga, Ontario, Canada
[b]Atomic Energy of Canada Limited, Montreal, Quebec, Canada
(shenwei@aecl.ca)

Abstract

A new flux-solver code named MINER Solver has been developed in order to overcome some of the built-in limitations of the RFSP core-analysis code. The MINER code includes both a finite-difference solver and a nodal method solver. Both solvers have multi-group capabilities with ADFs (Assembly Discontinuity Factors). The MINER code can be used independently to solve benchmark problems, or can be used with RFSP to solve full-core problems. In this paper, the accuracy of the MINER code is demonstrated by using it to solve a set of standard benchmark problems with both the FDM (Finite-Difference Method) and the nodal method.

1. Introduction

The RFSP core-analysis code [1] and its previous incarnations have been the primary reactor core-analysis tools in the Canadian nuclear industry for decades. However, the RFSP code has many built-in limitations. One of the limitations is that RFSP has no other flux solver than the finite-difference solver. In addition, the flux solver can handle 2-group problems but not general multi-group problems. Furthermore, the flux equations contain no ADFs (Assembly Discontinuity Factors) as part of the lattice properties.

In order to overcome these limitations of RFSP, the MINER (Multigroup Iterative Neutronics External Replacement) Solver was developed. The MINER code includes both a finite-difference [2] solver and a nodal-method [3] solver. Either solver can solve multi-group problems, with and without ADFs. The MINER solvers can be used independently to solve standard benchmark problems, or can be used with RFSP to solve full-core problems based on the RFSP input file.

The MINER Solver and its newly developed capabilities such as ADFs [4][5] were developed in anticipation of the future need of next-generation analysis tools that will be of significant importance to CANDU[2] applications. In this paper, the primary features of the MINER Solver are described, and the accuracy of the MINER Solver is demonstrated by using it to solve a set of standard benchmark problems with both the FDM (Finite-Difference Method) and the nodal method. The multi-group diffusion equation for the FDM and the nodal method

[1] © Atomic Energy of Canada Limited, 2009
[2] CANDU is a registered trademark of Atomic Energy of Canada Limited (AECL).

is outlined very briefly in Section 2. The primary features of the MINER code are described in Section 3. A set of benchmark problems were analysed and the results are discusses in Section 4. Conclusions are stated in Section 5.

2. The Multi-group Diffusion Equation for the FDM and the Nodal Method

By partitioning the Cartesian system into K homogeneous nodes V^k, k=1,2,…,K, the G-group three-dimensional (3-D) steady-state neutron-diffusion equation is written in the standard form:

$$\sum_{u=x,y,z} \frac{\partial}{\partial u} J_{gu}^k(\vec{r}) + \Sigma_{rg}^k \phi_g^k(\vec{r}) = Q_g^k(\vec{r}) \tag{1a}$$

where

$$\vec{r} = (x,y,z);\ u = x,y,z;\ g = 1,\ldots,G;\ k = 1,\ldots,K$$

and

$$Q_g^k(\vec{r}) = \frac{\chi_g^k}{\lambda} \sum_{g'=1}^{G} (\nu\Sigma_f)_{g'}^k \phi_{g'}^k(\vec{r}) + \sum_{\substack{g'=1 \\ g'\neq g}}^{G} \Sigma_{gg'}^k \phi_{g'}^k(\vec{r}) \tag{1b}$$

By using Fick's Law, the u-direction net neutron current can be expressed as:

$$J_{gu}^k(\vec{r}) = -D_g^k \frac{\partial}{\partial u} \phi_g^k(\vec{r}) \tag{1c}$$

Integrating Equation (1) over spatial node V^k with homogenized properties, and with half-widths a_x^k, a_y^k, a_z^k, we obtain the well-known nodal balance equation, which we write in terms of the surface-average currents $J_{gu}^k(\pm a_u^k)$ as follows:

$$\sum_{u=x,y,z} 2a_v^k 2a_w^k \left[\bar{J}_{gu}^k(a_u^k) - \bar{J}_{gu}^k(-a_u^k)\right] + \Sigma_{r,g}^k \bar{\phi}_g^k V^k = \bar{Q}_g^k V^k \tag{2a}$$
$$u,v,w = x,y,z;\ u \neq v \neq w;\ g = 1,\ldots,G;\ k = 1,\ldots,K$$

where the node volume-average flux and source are defined as:

$$\bar{\phi}_g^k = \frac{1}{V^k} \int_{-a_x^k}^{+a_x^k} dx \int_{-a_y^k}^{+a_y^k} dy \int_{-a_z^k}^{+a_z^k} \phi_g^k(\vec{r})\, dz \tag{2b}$$

$$\bar{Q}_g^k = \frac{1}{V^k} \int_{-a_x^k}^{+a_x^k} dx \int_{-a_y^k}^{+a_y^k} dy \int_{-a_z^k}^{+a_z^k} Q_g^k(\vec{r})\, dz$$
$$= \frac{\chi_g^k}{\lambda} \sum_{g'=1}^{G} (\nu\Sigma_f)_{g'}^k \bar{\phi}_{g'}^k + \sum_{\substack{g'=1 \\ g'\neq g}}^{G} \Sigma_{gg'}^k \bar{\phi}_{g'}^k \tag{2c}$$

and $V^k = 2a_u^k\, 2a_v^k\, 2a_w^k$ represents the volume of node k.

The surface-average current over the node surface at $u = \pm a_u^k$, is given by:

$$\bar{J}_{gu}^k(\pm a_u^k) = \frac{1}{2a_v^k}\frac{1}{2a_w^k}\int_{-a_v^k}^{a_v^k} dv \int_{-a_w^k}^{a_w^k} dw J_{gu}^k(\pm a_u^k, v, w) \tag{2d}$$

The solution of Equation (2a) requires additional equations relating the surface-average currents to the node volume-average fluxes. These additional coupling relationships are characterizing the various schemes that have been developed over the years for the solution of the neutron-diffusion equation.

One of the simplest means of obtaining these relationships is the well-known mesh-centred FDM approximation as adopted in the RFSP code. A more complicated means of obtaining these relationships is the modern nodal method. The nodal method has been used for light-water reactor (LWR) core-physics and safety analysis for several decades. Among the numerous advanced nodal methods, the Green's Function Nodal Expansion Method (GNEM) [3] is selected as a candidate nodal method in MINER for its efficiency and accuracy. The detailed formulation of GNEM can be found in [3].

During the derivation of the formulations for both the FDM and nodal method, ADFs are used to modify the flux-continuity condition at the lattice-cell interface by using the following equation:

$$f_{i-1}^{+}\phi_{i-1}^{+} = f_i^{-}\phi_i^{-} \tag{3}$$

Using this equation results in more general coefficients in the leakage term of the neutron-flux diffusion equation.

3. Main features of MINER

The MINER code has been developed to solve the multi-group diffusion equation, using both the finite-difference formalism and the nodal method formalism as described in Section 2. The primary features of MINER are:

- Solves NG-group diffusion problems, where NG may be any integer;
- Couples with RFSP to solve full-core problems based on the RFSP input file;
- Works for 1D, 2D, and 3D Cartesian problems;
- Uses the finite-difference method or the nodal method;
- Solves problems with or without ADFs (Assembly Discontinuity Factors) in both the finite-difference method and the nodal method;
- Programmed with FORTRAN-90/95; and
- Uses the data management based on HDF5 (Hierarchical Data Format) [15].

4. Preliminary numerical benchmark results

The accuracy of the MINER Solver is demonstrated by using it to solve a set of benchmark problems with both the FDM and the nodal method. The set of benchmark problems was chosen to contain some 2-group PWR (Pressurized Water Reactor) problems with and without ADFs, one 2-group CANDU problem in 2-D and 3-D, and one multi-group fast-reactor problem.

For all benchmarks, the FDM was run with a fine mesh of 16×16 sub-meshes/lattice, plus coarser meshes of 8×8, 4×4, 2×2, and 1×1 sub-meshes/lattice. The nodal method was run with the coarse mesh of 1×1 sub-meshes/lattice. For all benchmark problems, the normalized assembly/channel power densities and eigenvalue calculated with the 16×16 FDM are expected to be the most accurate and used as the reference solutions. The accuracy of the coarser meshes is expected to decrease with decreasing mesh size. The coarse-mesh (1×1) nodal results are as accurate as the fine-mesh (such as 8×8 or 16×16) FDM results. The relative difference in the normalized assembly/channel power densities reported in this section is defined as:

$$\varepsilon_j = \left\{ \frac{P_j^{miner} - P_j^{ref}}{P_j^{ref}} \right\} \times 100\% \tag{4}$$

where P_j^{miner} is the MINER-calculated normalized assembly/channel power densities at assembly/channel location j and P_j^{ref} is the reference (16×16 FDM) normalized assembly/channel power densities at assembly/channel location j.

4.1 2-D 2-group BIBLIS PWR benchmark problem

The first benchmark is a realistic commercial operating PWR problem, typically used in nodal method development [6][7]. It represents a fuel region surrounded by reflector and the base mesh spacing is 23.1226 cm per assembly. The large assembly size and the checkerboard fuel-assembly loading pattern make the problem hard to solve accurately. This problem has eight-fold symmetry, and so the results for only one-eighth of the reactor core are given.

The results obtained for this benchmark problem are shown in Figure 1. Compared to the reference solutions (16×16 FDM results), the accuracy of the FDM falls off quite quickly with decreasing mesh size, which is expected for a PWR-type reactor. The coarse-mesh (1×1) nodal results are about as accurate as the fine-mesh (such as 8×8 or 16×16) FDM results. The MINER results are as expected for FDM and nodal methods. The eigenvalue result for 1×1 GNEM and 16×16 FDM are compared to the numerical solution obtained in reference [7] in Table 1. The MINER results are very close to the expected eigenvalue for this benchmark. The benchmarking results confirm that both the FDM and the nodal method solvers have been correctly implemented in MINER in 2-D and 2-group form.

4.2 2-D 2-group EPRI benchmark problem

This benchmark is a simplified 2-D 2-group benchmark problem [8][9] used to validate the capability of applying the discontinuity factors in MINER. It represents a fuel region surrounded by reflector and the base mesh spacing is 21.0 cm per assembly. The benchmark results are available for calculations with and without ADFs. This problem has eight-fold symmetry, and so the results for only one-eighth of the reactor core are given.

The results obtained for this benchmark without and with ADFs are shown in Figure 2 and Figure 3, respectively. The results show that the inclusion of the ADFs has some impact on the eigenvalue (about 1.5mk) and power distribution (about 3%). The MINER results are as expected for FDM and nodal methods. For both cases with and without ADFs, the same observations and conclusion as above for the previous BIBLIS benchmark problem can be made. The eigenvalue results for 1×1 GNEM and 16×16 FDM are compared to the numerical solution obtained in reference [9] in Table 1. The MINER results are very close to the expected eigenvalue for this benchmark. The benchmark results confirm that the ADFs have been correctly implemented in both the FDM and the nodal method solvers of MINER.

4.3 2-D/3-D 2-group CANDU benchmark problem

This benchmark is a simplified CANDU core with only two fuel regions (inner and outer fuel regions) in the core, surrounded by a heavy-water reflector [10] [11]. This problem has eight-fold symmetry, and so the results for only one-eighth of the reactor core are shown.

The results obtained for the 2-D 2-group CANDU benchmark problem are shown in Figure 4. As opposed to the PWR benchmarks, the accuracy of the FDM falls off quite slowly with decreasing mesh size compared to the reference solutions (16×16 FDM results). The accuracy of the coarse-mesh (2×2) FDM is still quite good. The advantage of the fine-mesh FDM or the coarse-mesh (1×1) nodal method over the coarse-mesh FDM for a CANDU-type reactor is not as significant as that observed for a PWR-type reactor.

The channel power densities obtained for the 3-D 2-group CANDU benchmark problem are shown in Figure 5. The same observations and conclusion as above for the 2-D 2-group CANDU benchmark problem can be made. The eigenvalue results for 1×1 GNEM and 16×16 FDM are compared to the numerical solution obtained in reference [11] in Table 1. The MINER results are very close to the expected eigenvalue for this benchmark. The benchmark results confirm that both the FDM and the nodal method solvers have been correctly implemented in MINER for 3-D geometry.

4.4 2-D 4-group LMFBR benchmark problem

This benchmark is a 2-D 4-group LMFBR (Liquid Mental Fast Breeder Reactor) benchmark problem [12][13]. It represents two core regions surrounded by 2 blanket regions with a reflector. The benchmark is designed with 4-group properties. This problem has 4-fold symmetry, and so results of one-quarter of the reactor core are given.

The results obtained for this benchmark problem are shown in Figure 6. The numerical convergence of the results is as expected: the FDM accuracy increases with the mesh number increasing. The coarse-mesh (1×1) nodal results are about as accurate as the fine-mesh (such as 8×8 or 16×16) FDM results. The eigenvalue results for 1×1 GNEM and 16×16 FDM are compared to the numerical solution obtained in reference [12] in Table 1. The MINER results are very close to the expected eigenvalue for this benchmark. The benchmark results confirm that the multigroup diffusion equations have been adequately implemented in MINER.

5. Conclusion

The MINER code has been developed in order to overcome the built-in limitations of RFSP. The MINER code includes both a finite-difference solver and a nodal method solver in 2-D and 3-D Cartesian geometry. Both solvers have multi-group capabilities for solving problems of more than 2 groups, and have ADF capabilities as well. The accuracy of the MINER solver code has been demonstrated by using MINER independently to solve a set of standard benchmark problems. It is the first verification stage of MINER.

The MINER solver was developed in anticipation of the future need of next-generation analysis tools that will be of significant importance to CANDU applications. The MINER solver can thus be coupled to RFSP to solve the full-core problems based on the RFSP input file. In a second stage, the MINER results will be verified by comparing to its results with results from another code such as NESTLE [14] and RFSP. The MINER Solver could potentially serve as the flux solver for a next-generation reactor core analysis tool that will be developed to upgrade RFSP.

6. Acknowledgement

The authors wish to thank D.A Jenkins, D. Wren, P.G. Boczar, and M. Dahmani for their encouragement and advice in developing MINER.

7. References

[1] B. Rouben, “RFSP-IST, The Industry Standard Tool Computer Program for CANDU Reactor Core Design and Analysis”, Proceedings of the 13th Pacific Basin Nuclear Conference, Shenzhen, China, Oct. 21-25, 2002.

[2] W.M. Stacey, “Nuclear Reactor Physics”, John Wiley & Sons, Inc. (2001), pp. 81-87.

[3] Wei Shen, Zhongsheng Xie, and Banghua Yin, “The Green’s Function Nodal Expansion Method for Light Water Reactor Diffusion Calculations”, Nuclear Science and Engineering, **121**, 130-135 (1995).

[4] K. S. Smith, “Assembly Homogenization Technique for Light Water Reactor Analysis”, Prog. Nucl. Energy, **17**, (1986).

[5] K. Koebke, "Advances in Homogenization and Dehomogenization", International Topical Meeting on Advances in Mathematical Methods for the Solution of Nuclear Engineering Problems, Munich, **2**, 27-29, April 1981.

[6] K.S. Smith, "An Analytical Nodal Method For Solving The Two-Group, Multi-Dimensional, Static And Transient Neutron Diffusion Equations", M.Sc. Thesis, Massachusetts Institute of Technology, 1979.

[7] E.Z. Muller and Z.J. Weiss, "Benchmarking with the Multigroup Diffusion High-Order Response Matrix Methd", Ann. Nucl. Energy, Vol. 18, No. 9, pp535-544, 1991.

[8] W. Shen and H.B. Choi, "Application of Non-Linear Iterative Nodal Expansion Method for CANDU Analysis (Part I: Derivation of the Steady-State Nodal Diffusion Formulation)", Proceedings of the 21st Annual Conference of Canadian Nuclear Society, Toronto, June 11-14, 2000.

[9] H.S. Khalil, "The Application of Nodal Methods to PWR Analysis", Ph.D. Thesis, Massachusetts Institute of Technology, 1983.

[10] National Energy Software Center, "Benchmark Problem Book", ANL-7416, Argonne National Laboratory, 1985.

[11] J. Mao and J. Koclas, "The Analytic Nodal Method for CANDU Reactor Three-Dimensional Space-Time Kinetics Calculations", Proceedings of the 21st Annual Conference of Canadian Nuclear Society, Toronto, June 11-14, 2000.

[12] H.G. Kaper, G.K. Leaf, and A.J. Lindeman, "A Timing Comparison Study for Some High Order Finite Element Approximation Procedures and a Low Order Finite Difference Approximation Procedure for the Numerical Solution of the Multigroup Neutron Diffusion Equation", Nuclear Science and Engineering, **49**, 27-48, 1972.

[13] H.G. Kaper, G.K. Leaf, and A.J. Lindeman, "Applications of Finite Element Methods in Reactor Mathematics, Numerical Solution of the Neutron Diffusion Equation", ANL-7925, Argonne National Laboratory, 1972.

[14] P.J. Turinsky, "NESTLE, A Nodal Kinetics Code", Trans. Am. Nucl. Soc., Vol. 68, pp 432, 1993.

[15] The HDF Group, "HDF4 Reference Manual," Hierarchical Data Format (HDF) Software Library and Utilities, http://www.hdfgroup.org/doc.html.

Table 1- Comparison of MINER results to Benchmark Eigenvalues

	2-D 2-group BIBLIS	**2-D 2-group EPRI with ADF**	**3-D 2-group CANDU**	**2-D 4-group LMFBR**
MINER FDM 16×16	1.025129	0.926281	1.003702	1.057010
MINER GNEM 1×1	1.025298	0.926693	1.003727	1.056994
Published Results	1.025110[3]	0.926423[4]	1.003550[5]	1.056996[6]

[3] Value taken from [7]
[4] Value taken from [9]
[5] Value taken from [11]
[6] Value taken from [12].

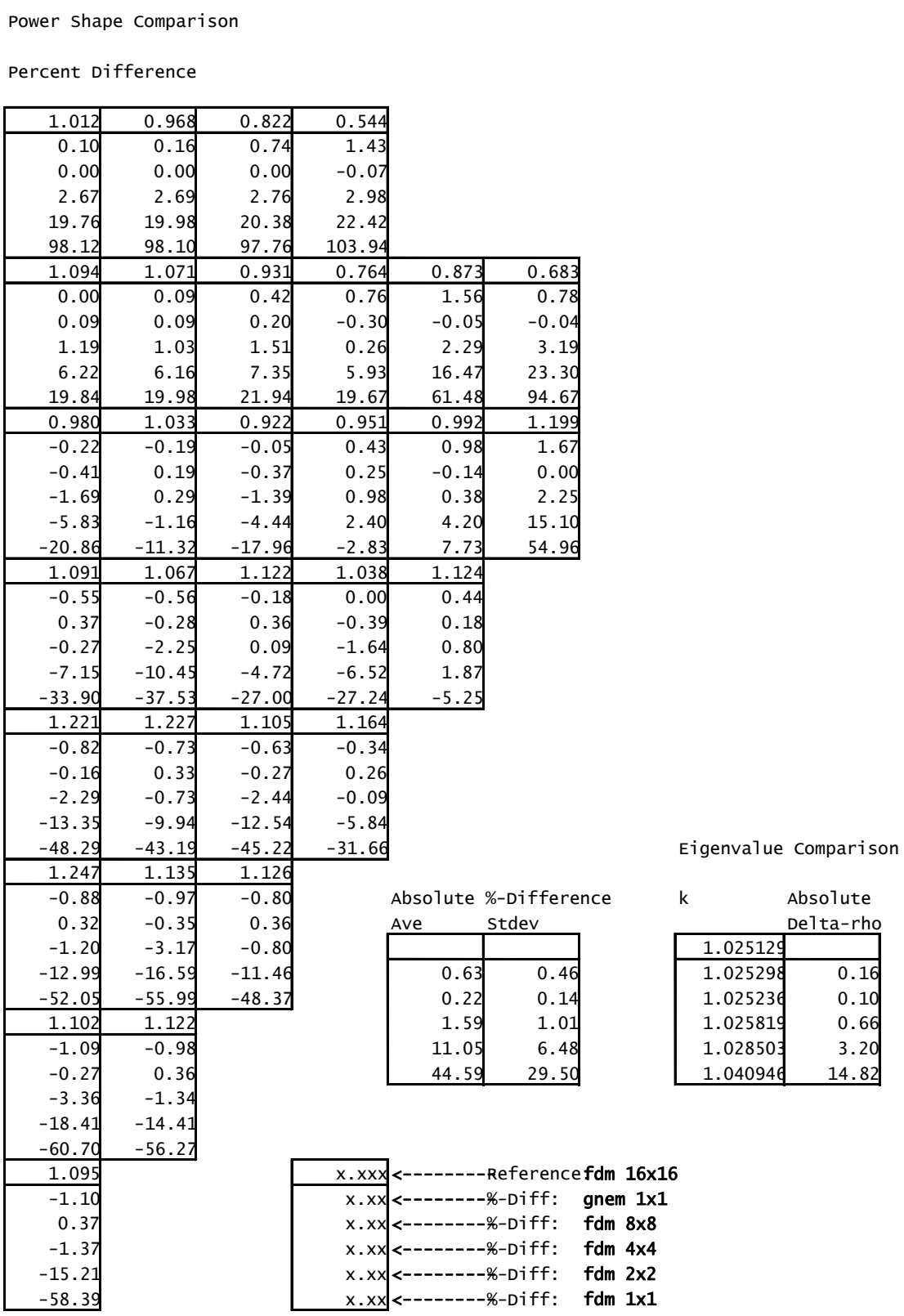

Figure 1 Normalized assembly power densities and percent differences for the 2-D 2-group Biblis PWR benchmark problem

Power Shape Comparison

Percent Difference

0.863	0.642
0.19	-0.14
-0.28	-0.58
-0.41	-0.98
1.39	2.02
8.26	14.97
1.196	1.190
-0.08	0.00
0.33	0.00
0.59	0.08
-1.00	0.50
-7.69	2.18
1.408	
0.00	
0.36	
0.36	
-2.34	
-12.64	

Absolute %-Difference

Ave	Stdev
0.08	0.08
0.31	0.21
0.48	0.33
1.45	0.75
9.15	4.94

Eigenvalue Comparison

k	Absolute Delta-rho
0.927867	
0.927972	0.12
0.927658	0.24
0.927629	0.28
0.929369	1.74
0.936030	9.40

x.xxx	<-------- Reference:	**fdm 16x16**
x.xx	<-------- %-Diff:	**gnem 1x1**
x.xx	<-------- %-Diff:	**fdm 8x8**
x.xx	<-------- %-Diff:	**fdm 4x4**
x.xx	<-------- %-Diff:	**fdm 2x2**
x.xx	<-------- %-Diff:	**fdm 1x1**

Figure 2 Normalized assembly power densities and percent differences for the 2-D 2-group EPRI benchmark problem without ADFs

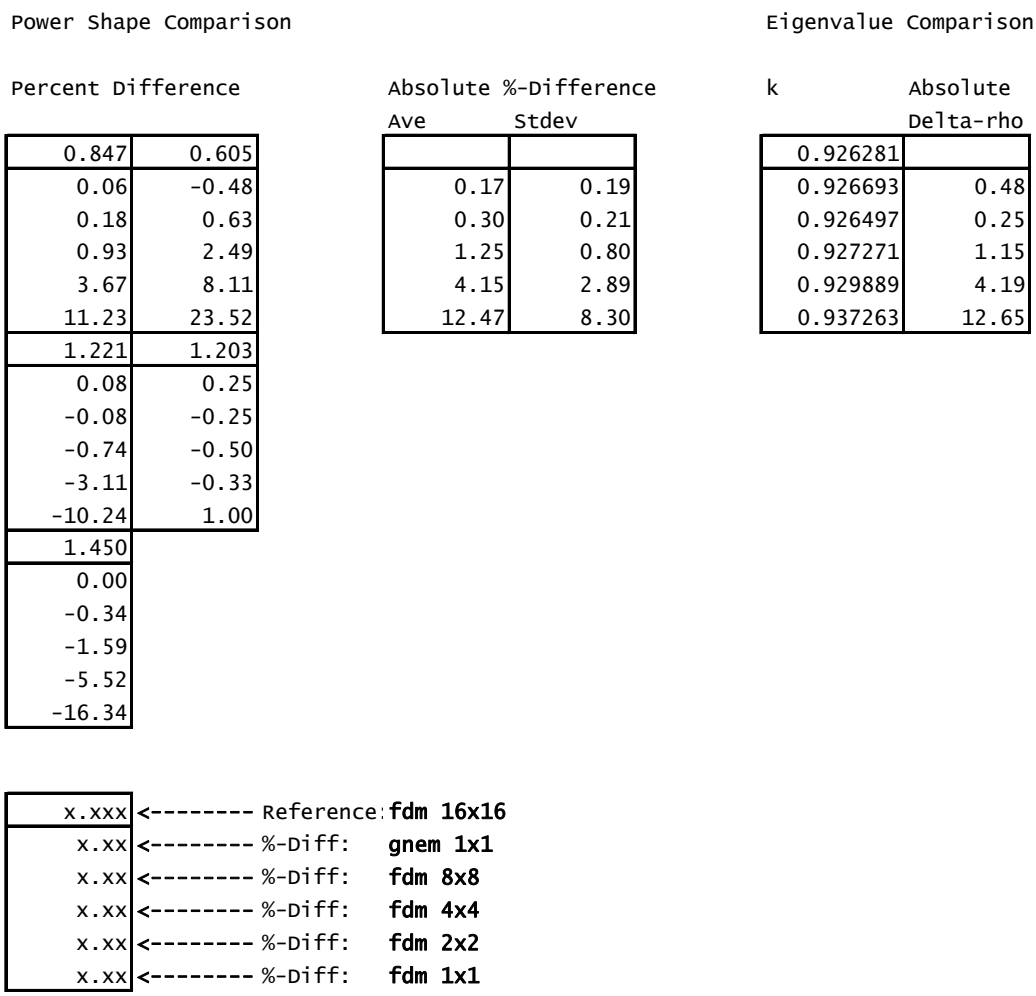

Figure 3 Normalized assembly power densities and percent differences for the 2-D 2-group EPRI benchmark problem with ADFs

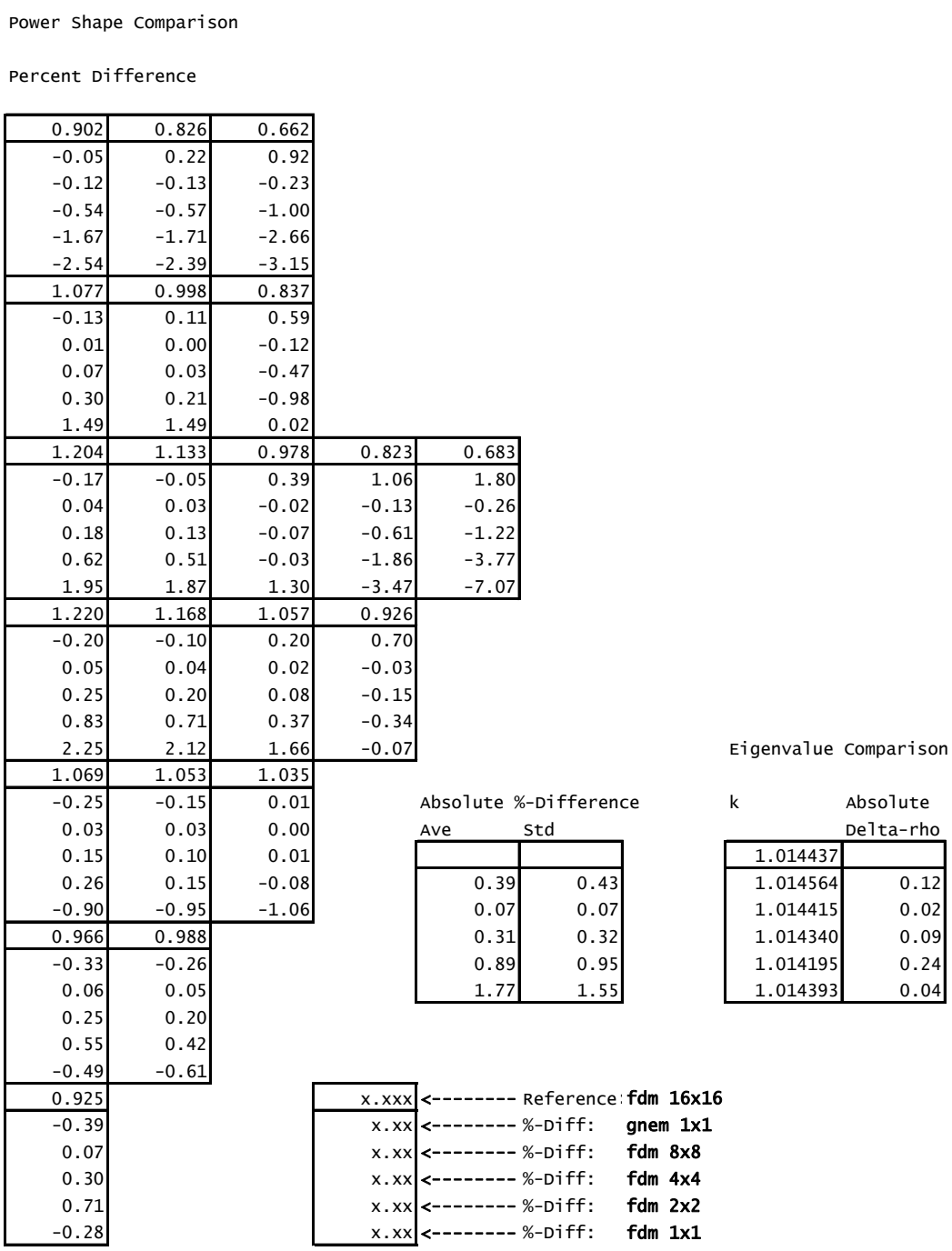

Figure 4 Normalized channel power densities and percent differences for the 2D CANDU benchmark problem

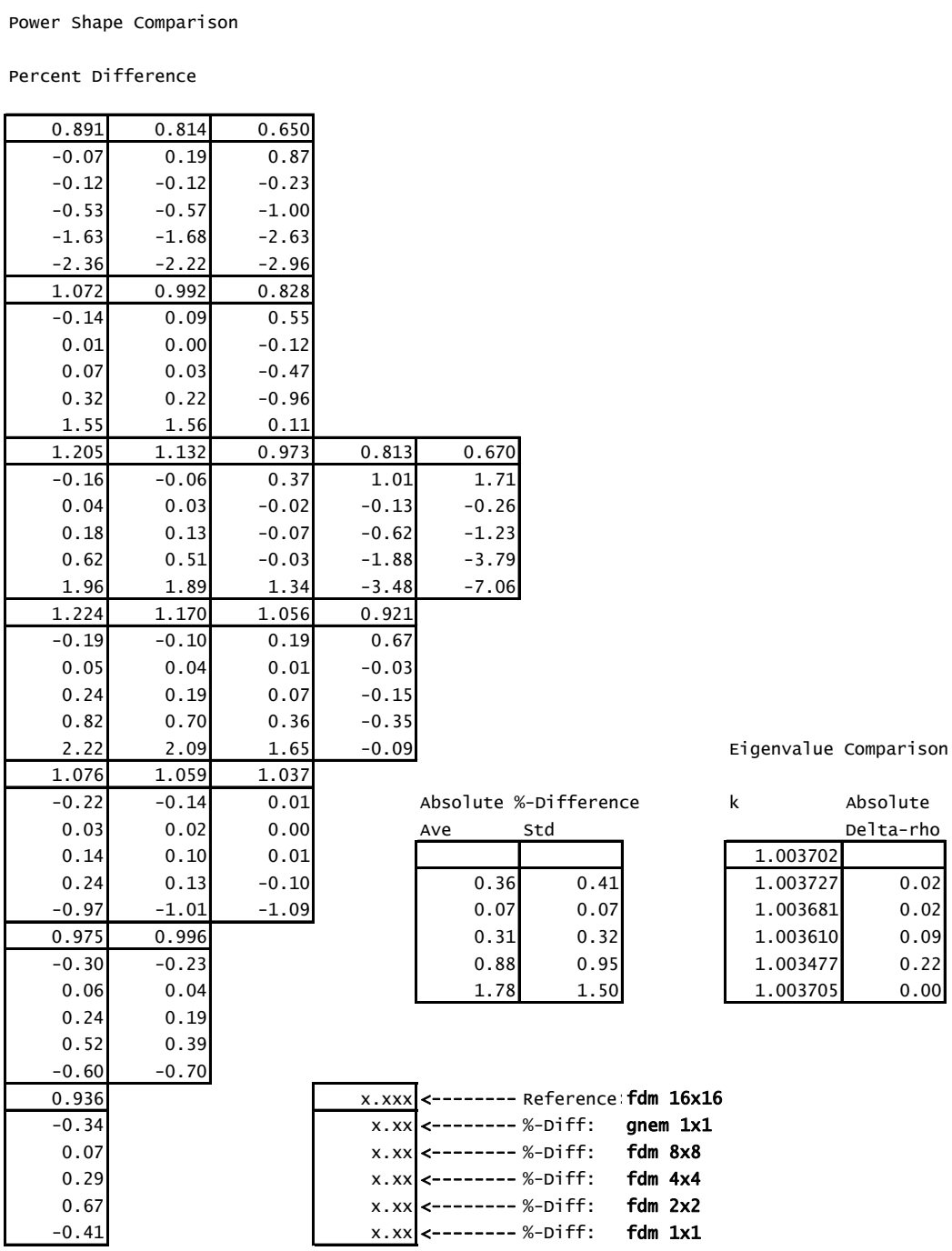

Figure 5 Normalized channel power densities and percent differences for the 3D CANDU benchmark problem

Power Shape Comparison

Percent Difference

0.095	0.082	0.060	0.039	0.025	0.016
0.04	0.02	0.04	0.01	-0.04	-0.14
-0.03	-0.03	-0.04	-0.06	-0.08	-0.09
-0.15	-0.14	-0.19	-0.27	-0.36	-0.44
-0.61	-0.59	-0.75	-1.13	-1.48	-1.79
-2.35	-2.22	-2.63	-4.54	-5.79	-6.83
0.184	0.158	0.112	0.068	0.041	0.024
0.04	0.03	0.02	0.01	0.00	-0.18
-0.03	-0.03	-0.04	-0.06	-0.07	-0.08
-0.17	-0.16	-0.17	-0.28	-0.35	-0.40
-0.70	-0.64	-0.67	-1.19	-1.46	-1.63
-2.67	-2.40	-2.25	-4.92	-5.66	-6.19
0.372	0.318	0.218	0.119	0.064	0.035
0.02	0.03	-0.01	0.13	0.05	-0.11
-0.07	-0.07	-0.06	-0.08	-0.07	-0.07
-0.34	-0.32	-0.27	-0.39	-0.34	-0.36
-1.38	-1.30	-1.03	-1.66	-1.41	-1.47
-4.84	-4.50	-3.40	-6.45	-5.42	-5.52
1.895	1.618	1.114	0.125	0.060	0.031
-0.01	-0.01	0.00	0.08	0.08	0.11
0.03	0.03	0.04	-0.11	-0.06	-0.06
0.15	0.17	0.19	-0.52	-0.30	-0.29
0.62	0.70	0.82	-1.94	-1.19	-1.16
2.61	2.97	3.65	-5.96	-3.98	-4.10
2.445	2.086	1.430	0.161	0.075	0.037
0.00	0.00	-0.01	-0.01	0.01	0.10
0.02	0.03	0.03	-0.12	-0.07	-0.06
0.11	0.13	0.16	-0.60	-0.32	-0.30
0.46	0.55	0.70	-2.31	-1.26	-1.19
1.89	2.26	3.07	-7.21	-4.28	-4.19
2.819	2.406	1.651	0.186	0.086	0.043
0.01	0.00	-0.01	0.06	0.04	0.04
0.01	0.02	0.02	-0.13	-0.08	-0.07
0.07	0.09	0.12	-0.64	-0.37	-0.33
0.28	0.37	0.51	-2.43	-1.46	-1.32
1.18	1.56	2.35	-7.71	-4.97	-4.74
2.514	2.147	1.478	0.206	0.099	0.050
0.00	0.00	-0.01	0.06	0.04	0.03
0.00	0.01	0.01	-0.12	-0.07	-0.06
0.01	0.03	0.06	-0.59	-0.33	-0.28
0.02	0.11	0.27	-2.32	-1.32	-1.14
-0.08	0.30	1.14	-7.78	-4.87	-4.31
2.709	2.316	1.601	0.224	0.109	0.056
0.00	0.00	0.00	0.01	0.01	0.04
-0.01	0.00	0.00	-0.13	-0.08	-0.07
-0.03	-0.01	0.02	-0.63	-0.39	-0.35
-0.15	-0.07	0.07	-2.46	-1.57	-1.43
-0.80	-0.44	0.31	-8.37	-5.81	-5.43
2.806	2.400	1.660	0.232	0.113	0.058
0.00	0.00	0.00	0.04	0.02	0.02
-0.01	-0.01	0.00	-0.13	-0.08	-0.07
-0.05	-0.03	0.00	-0.64	-0.40	-0.37
-0.22	-0.14	0.00	-2.54	-1.65	-1.52
-1.09	-0.74	-0.01	-8.67	-6.12	-5.77

Absolute %-Difference

Ave	Stdev
0.03	0.04
0.05	0.04
0.26	0.18
1.06	0.68
3.88	2.30

Eigenvalue Comparison

k	Absolute Delta-rho
1.057010	
1.056994	0.01
1.057058	0.04
1.057254	0.22
1.058059	0.94
1.061454	3.96

x.xxx	<--- Reference:	fdm 16x16
x.xx	<--- %-Diff:	gnem 1x1
x.xx	<--- %-Diff:	fdm 8x8
x.xx	<--- %-Diff:	fdm 4x4
x.xx	<--- %-Diff:	fdm 2x2
x.xx	<--- %-Diff:	fdm 1x1

Figure 6 Normalized assembly power densities and percent differences for the 4-group LMFBR benchmark problem